17th International Conference on the Application of Computer
Science and Mathematics in Architecture and Civil Engineering
K. Gürlebeck and C. Könke (eds.)
Weimar, Germany, 12–14 July 2006

THREE–DIMENSIONAL MODELING OF CONCRETE WITH DAMAGE AND PLASTICITY

A. Heuer*

* *Institute for Statics and Dynamics of Structures, Technische Universität Berlin, Germany*
E-mail: andreas@statik.bv.tu-berlin.de

Keywords: 3-dimensional, damage, plasticity, time–dependent, concrete

.

Abstract. *The concrete is modeled as a material with damage and plasticity, whereat the viscoplastic and the viscoelastic behaviour depends on the rate of the total strains.*

Due to the damage behaviour the compliance tensor develops different properties in tension and compression.

There have been tested various yield surfaces and flow rules, damage rules respectively to their usability in a concrete model. One three–dimensional yield surface was developed from a failure surface based on the Willam–Warnke five–parameter model by the author.

Only one general uni-axial $\sigma - \epsilon$–curve is used for the numeric control of the yield surface. From that curve all necessary parameters for different strengths of concrete and different strain rates can be derived by affine transformations.

For the flow rule in the compression zone a non associated inelastic potential is used, in the tension zone a Rankine potential. Conditional on the time-dependent formulation, the symmetry of the system equations is maintained in spite of the usage of non-associated potentials for the derivation of the inelastic strains.

In case of quasi statical computations a simple viscoplastic law is used that is rested on an approach to Perzyna. The parameters of this law are selected such that there only exists a pseudo dependence on the strain rate.

In contrast to many other authors, $\dot{\lambda}$ is not only determined from the principle of equality of dissipation power in the uni-axial and the three-axial state of stress. This equality is modified by a factor that depends on the actual stress ratio and in comparison with the Kupfer experiments it implicates strains that are more realistic.

The implementation of the concrete model is conducted in a mixed hybrid finite element.

An example in the structural level is introduced for verification of the concrete model.

1 INTRODUCTION

In the last years the implementation of new norms for reinforced and non-reinforced concrete constructions cooperating with much more computation power and more intensive economic competition have induced greater demand and distribution of nonlinear arithmetic techniques.

Naturally, the usage of computational methods has great advantages. EC 2 and DIN 1045 allow calculating the stress resultants for design purposes by using theory of elasticity. Already if it involves linear elastic problems there are two edges:

- the structural analyst is able to predict complicated structures and to size them much more fast and with more safety in particular
- prior the engineer sometimes had to work with simple structural models, therefore he had got section properties for the reinforcement, which were very uneconomically.

You can say, that most of the FEM programs for the upper purposes are working save and solid nowadays, if they are operated by engineers with professional knowledge. If you speak with practical working engineers often the question is formulated, whether nonlinear models for materials like concrete will prevail in practise. Maybe, but should the solution of daily acting problems the range of application of these models? To these themes some practical experiences shall be discussed:

1. By means of elasticity theory it won't be possible to verify the extrem high forces the concrete in the zone of tendon anchorage assembly can resist. Even if the strength increase that is allowed in DIN 1045 and EC 2 due to confinement is exploited, arithmetical the values of the approval document normaly will not be reached.
2. By conventional procedures of analysis there is no way to declare the high shear forces, the headed studs of a composite beam can transfer. For instance the German technical rules for composite beams permit a shear force per stud for static load of 120 kN. If one try to verify this load in a truss model the studs are overloaded. The determination of the forces in compressive strut delivers no better result. For other means of establishing bond action between slab and beam it is difficult to find a simple static system anyway, thinking for Perfobond [28] strips.
3. A further problem is the determination of the punching resistance of nearly the edge or the corner of a plate. In [5] you can find the proposal to increase the numerical value of the forces from the column cab by 40 percent.

There are many other examples to be find where the three-dimensional behaviour of concrete plays an important role [9].

To get economical solutions for these kinds of problem extensive and expensive test programs have to be carried out. Here one important task of nonlinear three–dimensional concrete models is to settle:

1. in supporting test programs of civil engineering projects
2. investigation and explanation of phenomenons are occuring
3. in employment by finding reliable static models that can be handled simple enough and which are able to describe complicated facts.

2 MATERIAL PROPERTIES OF CONCRETE

Concrete is a heterogenous material that compounds from cement mortar and aggregate. Even before the loads are applied, the state of concrete is of complex residual stress. That state of stress is initiated by

- the temperature gradient due to flowing of hydration heat
- constraint stresses caused by prevention of strains from shrinking of the hardened cement paste initiated by the grains of aggregate
- occuring of damage zones from nonequal and insufficient compaction.

The greatly different behaviour in regions of compression and tension is mainly due to the brittle properties of the set cement paste. In the state of loading the concrete develops a highly nonlinear behaviour. Besides anisotropic properties emerge. That are results of changes in the texture of the material, like the formation of cracks in the structure of the cement mortar and the growth of micro-cracks between the grains of aggregate and the hardened cement paste.

Considering an uniaxial compression test, the micro-cracks in existence keep stable at first. Therefore approximately a linear elastic behaviour can be observed. Above the range of 30% to 40% of the compressive strength, a spreading of micro-cracks along the boundaries of the components of the material is recognized. The load-displacement-path begins to bend. By completing of macroscopic cracks the failure state in compression is reached. After that state the load is sloping. Investigations of van Mier, Reinhardt an van der Vlugt [29] [23] show, that the shape of the curve after collapse depends on the size of the specimen.

The tensile strength amounts about 10% of the compression strength. Here the dependence on the size of the specimen is much more greater. Because of localization in the crack-zone, it is not possible to find a general $\sigma - \varepsilon$–relationship. Therefore the fracture energy G_f (1) is defined. The determination of the fracture energy is very much sensitive, it results from the crack width w and the average tensile stress σ.

$$G_f = \int_0^x \sigma(w) dw \tag{1}$$

In cyclic loading tests a degradation of the elastic properties can be detected. The effect of degradation is much more greater if it is created by tensile stresses [23].

The Kupfer experiments [12], that were made to research biaxial stress states of concrete showed that there are differences in the normalized failure stress in dependence on the stress ratio. Moreover it is detected, that the dedicated failure strains are growing with the increasing of the normalized failure stress. From all these facts could be deduced, that the three–dimensional behaviour is coupled by contraction at first and by dilatancy when the failure of the specimen is reached. In figure 2 results of the Kupfer-Experiments are compared to calculations with the concrete model.
The experiments of van Mier [29] and of Schickert and Winkler [25] show that the ductility of concrete is coupled with an increasing of the strength by influence of a triaxial stress state. Under hydrostatic compressive stresses collapsing does not happen.

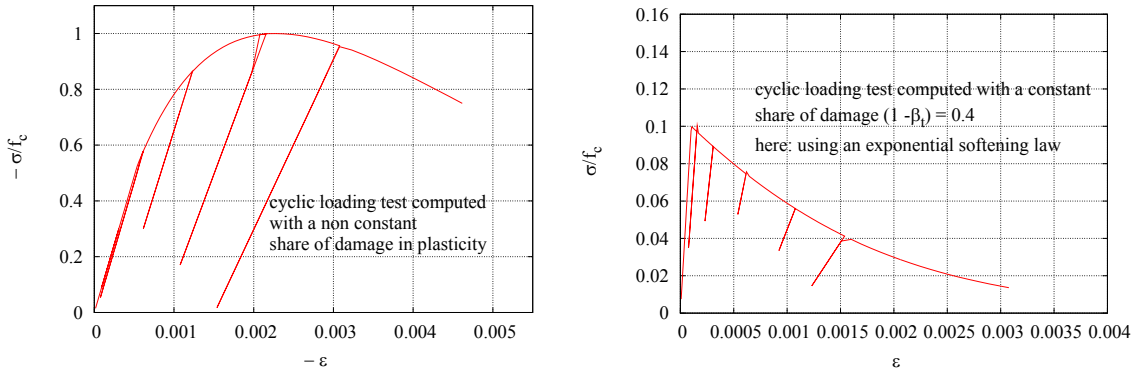

(a) compression (b) tension

Figure 1: cyclic loading tests

Concrete is a material, that responds highly to influences of the load velocity. Extensive investigations have been published to this topic [3] [6]. It is a fact that the strength of concrete increases by the strain rate. Beside you can detect that the stiffness increases depending on the velocity of loading. Several authors disagree about the strain ε_p, when the failure strength is reached. In the publications of Bazant [3] and Rasch [**?**] are propagated, that the failure strains decrease with the growth of the strain rate, Dilger [6] means, that the ε_p increases.

3 FORMULATION OF THE THREE–DIMENSIONAL CONCRETE MODEL

3.1 general considerations

From the second law of thermodynamics the Clausius-Duhem inequality follows as the dissipation power [14] [16] for an isothermal process:

$$\mathbb{D} = \frac{1}{2}\dot{\varepsilon}^d_{ij}\sigma_{ij} + \sigma_{ij}\dot{\varepsilon^p}_{ij} - X_{ij}\dot{\alpha}_{ij} - R\dot{r} \geq 0 \tag{2}$$

In this inequality $\underline{\varepsilon}^d$, $\underline{\varepsilon}^p$, r and $\underline{\alpha}$ are internal variables. The stress tensor $\underline{\sigma}$, the isotropic hardening, softening respectively R and the back stress tensor X_{ij}, that stands for the kinematic hardening are called the associated variables.

The inelastic strain $\dot{\underline{\varepsilon}}^{in}$ rate composes of the damage strain rate and the plastic strain rate, where β is a partitioning factor, that characterizes the ratio of damage and plasticity that is derived from an uniaxial cyclic loading test.

$$\dot{\varepsilon}^{in}_{ij} = \dot{\varepsilon}^d_{ij} + \dot{\varepsilon}^p_{ij} = (1-\beta)\dot{\varepsilon}^{in}_{ij} + \beta\dot{\varepsilon}^{in}_{ij} \tag{3}$$

It is postulated that the kinetic laws are derived from a potential of dissipation by introduction of a scalar multiplier $\dot{\lambda}$.

$$\dot{\varepsilon}^{in}_{ij} = \frac{\partial Q}{\partial \sigma_{ij}}, \qquad \dot{\alpha}_{ij} = -\frac{\partial Q}{\partial X_{ij}}, \qquad \dot{r} = -\frac{\partial Q}{\partial R} \tag{4}$$

The factor $\dot{\lambda}$ is a lagrangian multiplier from solving an optimizing problem if an associated flow-rule is used [8] [16].

3.2 Viscoplasticity

There are different approaches in modeling viscoplastic materials. The rheological description of materials is based on pure mechanical imaginations. For example time–dependent phenomenons like viscoelasticity can be explained with the well-known Maxwell-Model or the Kelvin-Voigt-Model, one model for viscoplasticity is that from Bingham [11].

Another strategy was suggested by Perzyna [18]. He gave the material law for a visco-plastic medium in the general form of 5.

$$\dot{\varepsilon}_{ij}^{p} = \Psi(F)\frac{\partial Q}{\partial \sigma_{ij}} \tag{5}$$

The function $\psi(F)$ can be determined from uniaxial experiments in connection with the yield function F.

One expression for the viscous stress comes from metal plasticity:

$$\sigma_u = K_v \langle \dot{\varepsilon}_v \rangle^{\frac{1}{N}} \tag{6}$$

Later this equation is used in the concrete model to stabilize the numeric expressions in the range of horizontal tangents. The yield condition, conditional on the occurrence of the viscous stress, is read:

$$F(\underline{\sigma}, \underline{X}, R) > 0 \tag{7}$$

.

3.3 Modeling concrete in compression

In this model only isotropic hardening in the compression zone is used. Therefore (2) reduces in consideration of (4) and (3) to:

$$\mathbb{D} = \frac{1}{2}\dot{\lambda}^{-}(1-\beta^{-})\frac{\partial Q^{-}}{\partial \sigma_{ij}}\sigma_{ij} + \dot{\lambda}^{-}\beta^{-}\frac{\partial Q^{-}}{\partial \sigma_{ij}}\sigma_{ij} - R\dot{r} \geq 0 \tag{8}$$

The multiplier $\dot{\lambda}^{-}$ follows from equivalence in the dissipation power of the triaxial and the uniaxial stress state. Here this equivalence is modified by a factor $f_m(\sigma_{ij})$ [17] [7].

$$\dot{\lambda} = \frac{\sigma_v^{-} f_m}{\frac{\partial Q^{-}}{\partial \sigma_{ij}}\sigma_{ij}}\dot{\varepsilon}_v^{-} = \frac{1}{\tau^{-}}\dot{\varepsilon}_v^{-} \tag{9}$$

, Here $\dot{\varepsilon}_v^{-}$ is the uniaxial equivalent strain and σ_v is the effective stress in compression.

In contrast to other publications [4] [20] [1] the factor f_m effects more realistic failure strains on the local material level. In case of practical computations of systems with hyperstatic bearing greater constraint stresses can be induced. The expression of f_m in figure 2(b) was derived from the Kupfer-Experiments. σ_1 and σ_2 are the stresses with the highest absolute values.

The inelastic strain rates

$$\dot{\varepsilon}_{ij}^{in-} = \dot{\varepsilon}_v^{-} A_{ij}^{-} \tag{10}$$

result from the definition:

$$A_{ij}^{-} = \frac{1}{\tau^{-}}\frac{\partial Q^{-}}{\partial \sigma_{ij}} \tag{11}$$

The effective stress can be written as:

$$\sigma_v^- = \frac{1}{f_m} A_{ij}^- \sigma_{ij} \tag{12}$$

With the expression $\dot{\varepsilon}_{ij}^d = \dot{F}_{ijkl}\sigma_{kl}$ the rate of the compliance tensor follows to:

$$\dot{F}_{ijkl}^- = \dot{\varepsilon}_v \frac{A_{ij}^- A_{kl}^-}{f_m \sigma_v^-} \tag{13}$$

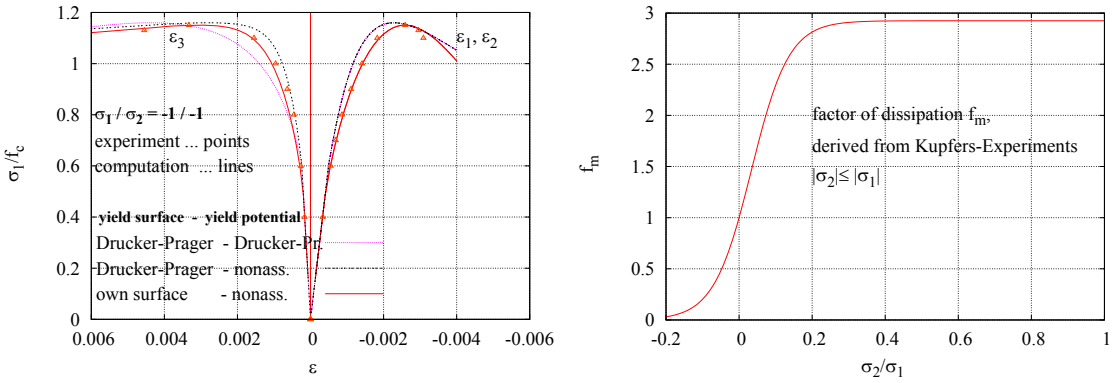

(a) Kupfer-experiments

(b) fm-curve

Figure 2:

3.4 Failure criterion and yield surface

Yield surfaces based on well-known von Mises-Criterion or the Drucker-Prager-Criterion are not suitable for three–dimensional modeling of Concrete. The second one often is used for two–dimensional theories. For a better approach in three-dimensional modeling here the Willam-Warnke failure criterion is used. The mathematical definition is given in Haigh-Westergard-coordinates [4], that are the hydrostatic stress $\sigma_m = \frac{I_1}{3}$ with the first invariant I_1 of the stress tensor, the radius $\rho = \sqrt{2}\sqrt{J_2}$ with the second invariant J_2 of the deviator and the Lode-angle θ comes from $\cos 3\theta = \frac{3\sqrt{3}}{2}\frac{J_3}{J_2^{\frac{3}{2}}}$, where J_3 is the third invariant of the stress deviator. In figure 3(a) you can realize the meaning of the three coordinates. Willam-Warnke made a quadratic approach for the hydrostatic stress addicted to the radius of the compression meridian ρ_c and the radius of the tension meridian ρ_t.

$$\sigma_m = a_0 f_c + a_1 \rho_t + a_2 \rho_t^2 \tag{14}$$

$$\sigma_m = b_0 f_c + b_1 \rho_c + b_2 \rho_c^2 \tag{15}$$

The compression meridian and the tension meridian have the same point of intersection on the hydrostatic axis, therefore $a_0 = b_0$ must be. The remaining coefficients follow from the tests for uniaxial compression and tension, biaxial compression and at least from two tests for combined biaxial compression. The radius $\rho_f(\theta)$ originate by connecting ρ_t and rho_c by the fourth path of an ellipse. So the failure surface is continuous and convex.

Now the yield surface can be constructed. The yield surface is controlled by the uniaxial $\sigma - \varepsilon^-$-curve, which is deduced from the general $\sigma - \varepsilon$-curve in a numerical way.

$$F(\sigma_{ij}, \sigma_m, \theta) = \rho(\sigma_{ij}) - k(\varepsilon_v^-, \sigma_m, \theta)\rho_f(\sigma_{ij}, f_c) \tag{16}$$

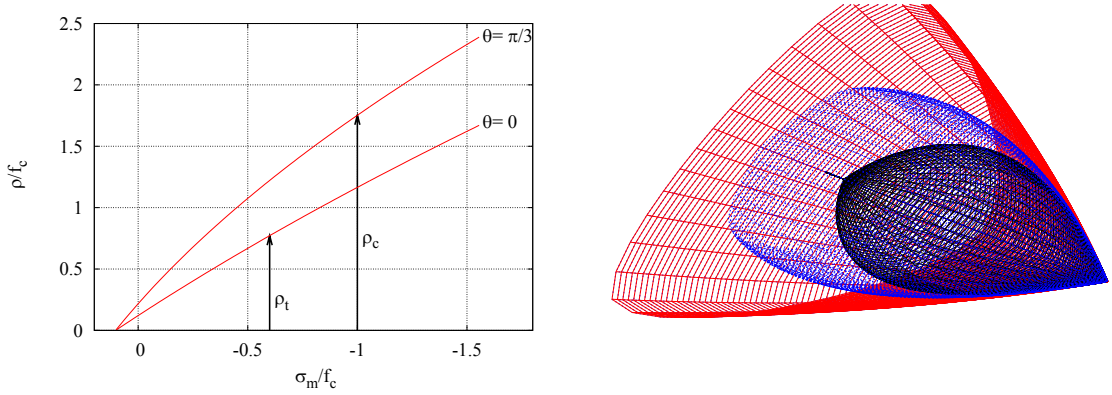

(a) meridians of tension and compression (b) failure surface–yield surfaces

Figure 3:

Concluding [4] the hydrostatic axis is divided into three sections. In section one and two k is approached by a quadratic formulation, in section three, the yield surface is closed by a cape. It is distinguished between k_t and k_c, therefore $k(\varepsilon_v^-, \sigma_m, \theta)$ is a linear relation between k_c and k_t. If the uniaxial failure strength is reached, the yield surface and the failure surface are identical.

For the stability of the numerical algorithm computation of the effective stress σ_v^- is crucial. This computation is made by affine contraction of the yield surface. In contrast to yield surfaces based on von Mises or Drucker-Prager criterion, this problem must be solved by numerical tools. The method of Regula-Falsi has been taken here. This method is not brilliant especially, but it is very reliable.

3.5 Flow rule in compression

Based on the time–dependent formulation of the concrete model, there are no difficulties with unsymmetrical matrices. Therefore it is no problem using different flow rules. At present there are three flow rules implemented. The first one is derived from a von Mises potential,

$$\dot{\varepsilon}_{ij}^{in-} = \dot{\lambda}\frac{1}{2J_2}\sigma_{ij}^D \tag{17}$$

here σ_{ij}^D is the second invariant of the stress tensor. If the flow rule is derived from a Drucker potential, it remains

$$\dot{\varepsilon}_{ij}^{in-} = \dot{\lambda}(\alpha\delta_{ij} + \frac{1}{2J_2}\sigma_{ij}^D) \tag{18}$$

The hydrostatic term α is a function of ε_v^- in the third flow rule. This flow rule creates the best results on the material level, if it is recombined with the yield surface developed here. Some results on the material level are shown in figure 2(a).

3.6 Modeling concrete in tension zone

The crack initiation in the tension zone is represented here by a kinematic softening phenomenon. This corresponds to a rotating smeared crack model. By means of the back stress tensor $\underline{X}$ later the cracks can be illustrated very well. Using the equations (2) and (4) and the principle of the equivalence of the dissipation power, simultaneous three multipliers for tension can be computed at most (19).

$$\dot{\lambda}^{+}_{(k)} = \frac{\sigma^{+}_{v(k)}}{\frac{\partial Q^{+}_{k}}{\partial \sigma_{ij}}(\sigma_{ij} - X_{ij})} \dot{\varepsilon}^{+}_{v(k)} \tag{19}$$

$$\sigma^{+}_{v(k)} = \Lambda_k(\underline{\sigma} - \underline{X}) \tag{20}$$

The definition for the effective stress corresponds to the k–th eigenvalue of the tensor $M_{ij} = \sigma_{ij} - X_{ij}$. The criterion for cracking is read:

$$F_{t(k)} = \Lambda_k - f_t > 0 \tag{21}$$

For calculating the evolution of the back stress the assumption is made, that the rate $\dot{X}_{ij}$ of the back stress only depends on the diagonal components of the internal variable α_{ij}, if this tensor is transformed to the system of coordinates, that results from the eigenvectors of $\underline{M}$. That leads to the equation:

$$\dot{\tilde{X}}^{(k)}_{(ii)} = \dot{\lambda}^{+}_{(k)} \frac{\partial \tilde{X}_{(ii)}}{\partial \tilde{\alpha}_{(ii)}} \tilde{M}^{(k)}_{(ii)} \tag{22}$$

Here $\tilde{}$ means, that the components refer to the system of principle axis of the tensor $\underline{M}$.

Normally, uniaxial softening laws are not derived from $\sigma - \varepsilon$-curves [17] [7], like in the compression zone often is done. Here uniaxial softening laws shall be given, from there it can be found the assigned $\sigma - \varepsilon$-curve, if it is needed. There are two parameters, affecting the shape of the softening law. That are the fracture energy G_f and the tensile strength f_t. The fracture energy of concrete is very small, sometimes that causes numerical problems. For example G_f can be taken from CEB-FIP-Model Code. Within an FEM-computation a softening law is constructed with help of the equivalent length (23) from these two parameters for every element, where V_f and A_f come from the dimensions of the volume element.

$$l_c = \frac{V_f}{A_f} \tag{23}$$

There can be found an extensive analyze of several softening laws in [16]. Here only the applied expressions shall be given.

Exponential softening law:

$$X(\varepsilon_v) = f_t(\exp(-\frac{\varepsilon^{+}_{v}}{\varepsilon_u}) - 1) \tag{24}$$

pure plasticity ($\beta^+ = 1$): pure damage ($\beta^+ = 0$):

$$\varepsilon_u = \frac{G_f}{l_c f_t (1 - \frac{1}{e})} \qquad (25) \qquad \varepsilon_u = \frac{2G_f}{l_c f_t (1 - \frac{1}{e})} \qquad (26)$$

Hyperbolic softening law:

$$X(\varepsilon_v^+) = -f_t \frac{1}{1 + \frac{\varepsilon_v^+}{\varepsilon_u}} \qquad (27)$$

pure plasticity ($\beta^+ = 1$): pure damage ($\beta^+ = 0$):

$$\varepsilon_u = \frac{G_f}{2 l_c f_t} \qquad (28) \qquad \varepsilon_u = \frac{G_f}{l_c f_t} \qquad (29)$$

In figure 1 the plot of an uniaxial cyclic loading test is drawn. The evolution of the compliance tensor, that is to realize in the deterioration of stiffness, to an expression, similar to (13).

3.7 Consideration of strain-rate effects

The most important assumption is the affinity of the $\sigma - \varepsilon$ -curves for various total strain-rates if strain-rate effects are considered. A general relation for the $\sigma - \varepsilon$ –curve has been taken from [15].

For transformation of the function from one to the other two values are necessary, the compressive strength f_{c1} dependent on the strain-rate and the peak strain ε_{cp1} assigned. The formula for the compressive strength has been taken from [3].

$$f_{c1} = f_{c0}(1.4 - 1.5 \frac{1 - \dot{\varepsilon}^{\frac{1}{8}}}{1.84 + 3.2 \dot{\varepsilon}^{\frac{1}{8}}}) \qquad (30)$$

Here, f_{c0} is the compressive strength from a compressive test with a total strain rate of $3.3 \dot{\varepsilon} 10^{-5} s^{-1}$ that corresponds to a statical test. The empirical expression for the assigned peak strain is given by Dilger [6].

$$\varepsilon_{cp1} = -(1.3 - 0.06 \lg \dot{\varepsilon} + 0.01 f_{c0}, \quad f_{c0}[N/mm^2] \qquad (31)$$

In [26] it is shown, that the effective strain rate $\dot{\varepsilon}$ in the equations (30) and (31) can be composed from

$$\dot{\varepsilon} = 0.9 \sqrt{\dot{\varepsilon}_{ij} \dot{\varepsilon}_{ij}} \qquad (32)$$

approximately.

Two curves are called affine, if they can be adjusted by horizontal and vertikal expanding (see figure 4). By the definitions

$$\beta_a = \frac{f_{c1}}{f_{c0}} \qquad (33)$$

$$\alpha_a = \frac{\varepsilon_{p0}}{\varepsilon_{p1}} \qquad (34)$$

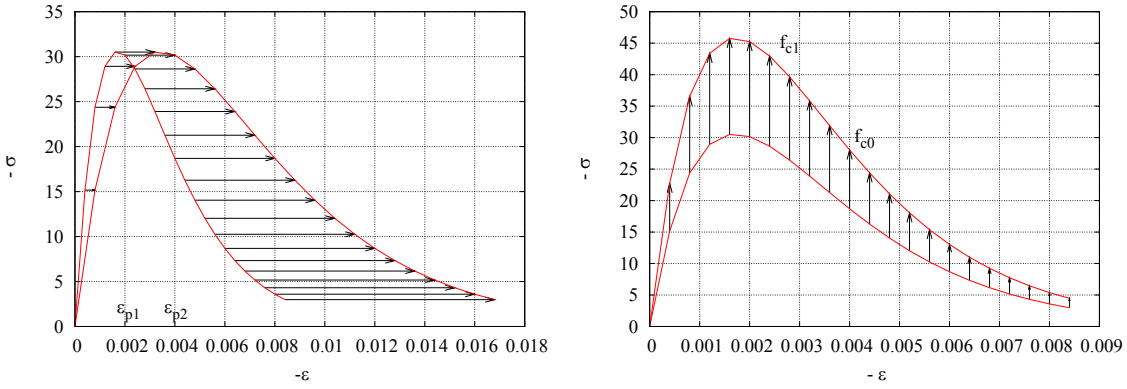

Figure 4: affine transformations

the transformation of the $\sigma - \varepsilon$ -curve is deduced to:

$$\sigma(\varepsilon, \dot{\varepsilon}) = \beta_a(\dot{\varepsilon})\sigma_0(\alpha_a(\dot{\varepsilon})\varepsilon) \tag{35}$$

For a constant damage parameter β (not have to be mistaken for β_a) the rate dependent compliance tensor is derived from the uniaxial stiffness to:

$$F_{ijkl}(\dot{\varepsilon}) = \frac{1}{\alpha_a(\dot{\varepsilon})\beta_a(\dot{\varepsilon})} F_{ijkl(0)} \tag{36}$$

The mathematical description for the uniaxial ultimate stress is deduced from the statical $\sigma_G - \varepsilon_v$-expression.

$$\sigma_G(\dot{\varepsilon}, \varepsilon_v) = \beta_a(\dot{\varepsilon})\sigma_{G0}(\alpha_a\varepsilon_v) \tag{37}$$

There is shown a comparison in figure 5 between the calculations of this theory and experimen-

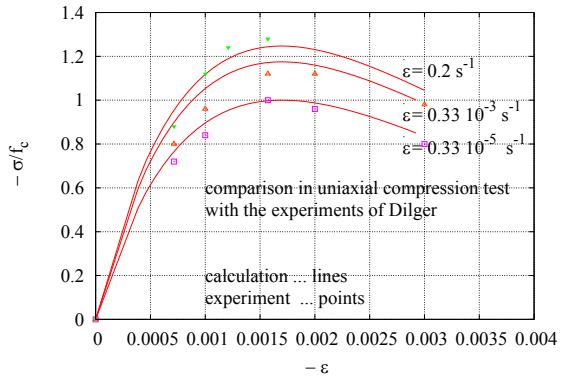

Figure 5: strain-rate-behaviour-of concrete

tal results of Dilger [6]. You can detect some differences in the peak stresses, that is why the peak stresses are from other tests [3], but the peak strains are from [6]. In figure 5 it is indicated well that in this theory the influence of the strain rate to the elastic stiffness is considered. .

4 USAGE OF THE CONCRETE MODEL

4.1 Annotations to the finite element concept and reinforcement

The model is implemented to a hybrid finite element. That element works with 8 nodes. In that concept, the material law can be interpreted as a constrained condition of a Lagrangian optimization problem [2] as opposed to the displacement method. Here the element matrices are derived by usage of principle of virtual forces and principle of virtual displacements simultaneous. On the system level the degrees of freedom for the forces are eliminated. Further details can be found in [10]

Dynamic equilibrium:

$$\int_{(G)} (\delta v_j \rho \dot{v}_j + \delta \dot{\varepsilon}_{kl} \sigma_{kl} - \delta v_j f_j) dV - \int_{(R)} \delta v_j t_{0j} dA = 0 \tag{38}$$

Compatibility:

$$\int_G [\delta \sigma_{ij} (\dot{\varepsilon}_{ij} - (1 - \langle I_1 \rangle) F^-_{ijkl} \dot{\sigma}_{kl} - \langle I_1 \rangle F^+_{ijkl} \dot{\sigma}_{kl} - \dot{\varepsilon}^-_v A^-_{ij} - \sum_{m=1}^{3} \dot{\varepsilon}^+_{v(m)} A^+_{ij(m)})] dV = 0 \tag{39}$$

Determination of the viscous stresses:

$$\int_{(G)} \delta \dot{\varepsilon}^-_v (\sigma^-_u - \sigma^-_v + \sigma^-_G) dV = 0 \tag{40}$$

$$\int_{(G)} \delta \dot{\varepsilon}^+_{v(m)} (\sigma^+_{u(m)} - \sigma^+_{v(m)} + f_t) dV = 0, \quad (m = 1, 2, 3) \tag{41}$$

For time discretization an approach is made similar a predictor-corrector procedure. The formulations for the element matrices are symmetrically, even if non associated flow rules are used.

The reinforcement is discretized with uniaxial hybrid strain elements. The geometrical properties are independent on the discretization of the volume elements. There has been implemented an automatical generation of reinforcement elements. Every point of intersection between the side faces of a volume element and a reinforcement bar causes three constraints of displacement. For the description of kinematic and isotropic hardening the approaches from Chaboche [14] are implemented.

$$X = X_\infty (1 - \exp(-\gamma \varepsilon_v)) \tag{42}$$

$$R = R_\infty (1 - \exp(-b \varepsilon_v)) \tag{43}$$

Where X_∞, R_∞, γ and b are material properties. The values for reinforcement of a usually rebar are piced as follows:
$R_\infty = 4kN/cm^2$, $b = 100, f_{yk} = 50kN/cm^2$, $f_{k0} = 48.5kN/cm^2$, $E = 20000kN/cm^2$, kinematic hardening is neglected here. Note, that f_{yk} is not a mean value. A comparison to DIN 1045 Abs. 9 is given in figure 6.

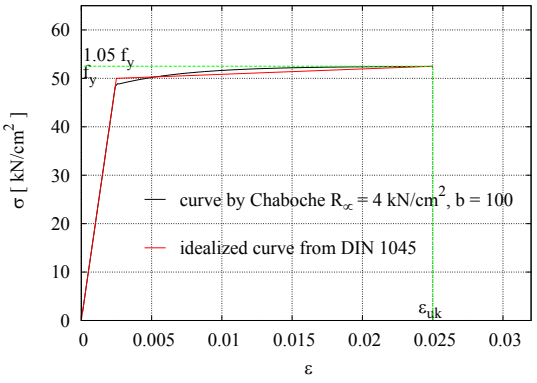

Figure 6: $\sigma - \varepsilon -$ curve of reinforcement

5 EXAMPLE CALCULATIONS

For example calculations a slightly reinforced frame is presented. This frame is a current project of our institute. During the next weeks tests for the statical and dynamical structural behaviour shall be made. Therefore precalculations were made by using the introduced concrete model. The material properties has been estimated.

In figure 8(b) the formation of cracks is indicated well. It is represented by the kinematic softening of the concrete. The localization of the cracks is recognized very well in spite of the usage of a smeared crack model.

The calculations had been carried out with different meshes, the results are similar. Figure 7 shows the path of the load-displacement relation. Here the charge of failure is to be seen clearly. It shall be emphasized, that no points of elements are switched off, if a certain limit (of stress or strains) is reached. The slope of the curve happens in a natural way, that is, if the softening of material points in compression or in tension develops. There can be seen a good convergence in computation of states that are nearly the theory of beams.

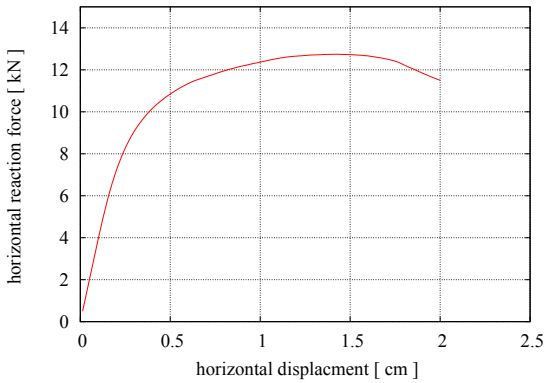

Figure 7: predicted load displacement path for the upper right frame corner

The quality of the results referring to the reality will have to be proved, when the experiments will be made. The predictions by a computer program, which disregards the tension zone of concrete shows a lower failure load. One calculation, that was made by the theory of

plastic hinges, where the resisting moments had been estimated from experiences from other calculations with slightly reinforced beams gave the result of 13.6 kN for the resisting force.

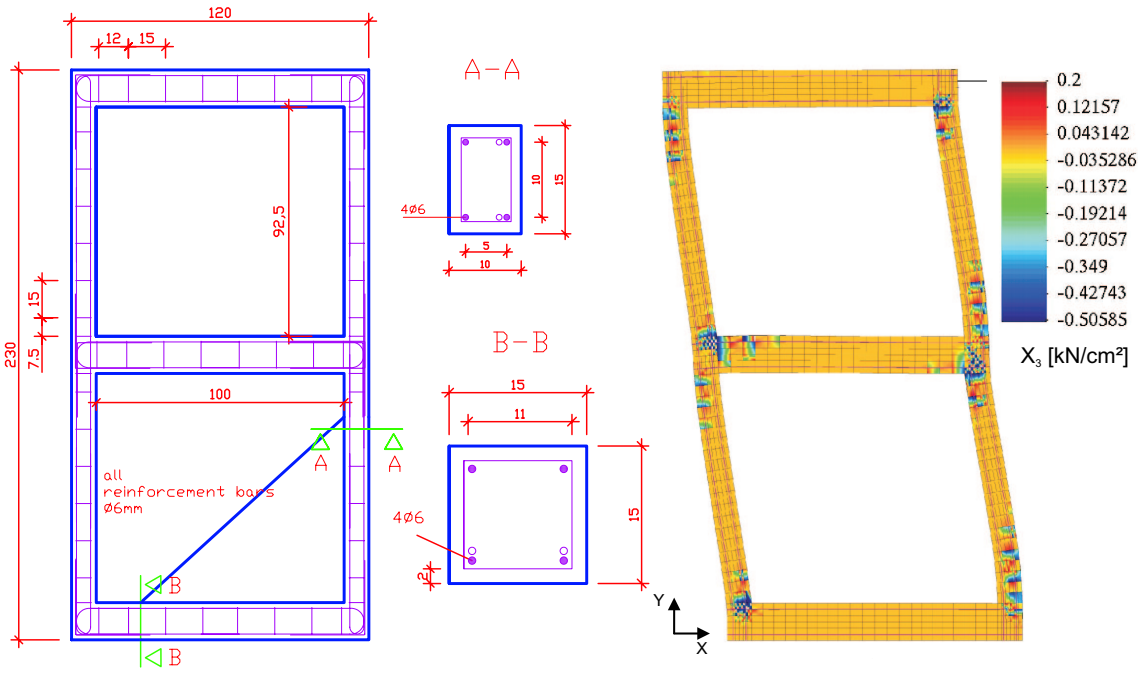

Figure 8: Vierendeel frame, estimated material parameters: concrete: $f_c = 4.03\ \ kN/cm^2$, $\varepsilon_{cp0} = 0.00217$ $f_t = 0.403\ \ kN/cm^2$, $G_f = 0.08 \cdot 10^{-2}\ \ kN/cm,\ \ \nu = 0.2$ (Poisson'ratio), partioning factors $\beta^+ = 0.6,\ \ \beta^- = 0.0$, steel $f_{yk} = 50\ \ kN/cm^2$

6 CLOSURE

A three–dimensional concrete model has been introduced. This model has viscoelastic and viscoplastic properties. The results in the material level are very well. Computations in the structural level show good convergence. For verification of the concrete model further calculations and adjustments in material parameters are required.

REFERENCES

[1] Alex, R.: Zeitabhängiges Plastizitäts- und Schädigungsmodell zur Berechnung von Tragwerken aus Stahlbeton unter statischen und dynamischen Einwirkungen. Dissertation, TU Berlin, 1999.

[2] Bathe, K. J.: Finite Elemente procedures in engineering analysis. Prentice-Hall, Inc., Englewood Cliffs, New Jersey 07632, 1982

[3] Z.P. Bazant, B.H. Oh.: Strain-Rate in rapid triaxial loading of concrete. J. Engng Mech. Div., ASCE, 108, p.764-782, 1982.

[4] Chen, W. F., Han, D. J.: Plasticity for Structural Engineers. Springer-Verlag New York, Berlin, Heidelberg 1988.

[5] DAfStb. Heft 240: Hilfsmittel zur Berechnung der Schnittgrößen und Formveränderungen von Stahlbetontragwerken nach DIN 1045, Ausgabe Juli 1988 - Seiten. Beuth, 1991.

[6] Dilger, W.H., Koch, Kowalczyk R.: Ductility of plain and confined concrete under different strain rates. Journal of the American Concrete Institute, January - February 1984.

[7] Golowin, A.: Überspannungskonzept zur Modellierung von duktil-spröden Deformationsprozessen in Stahlbeton Dissertation, Technische Universität Berlin, 2001.

[8] Govindjee, S., Kay, G., Simo, J.: Anisotropic modelling and numerical simulation of brittle damage in concrete. Int. J. Mumer. Meth. Engng., 38, S. 3611-3633, 1995

[9] Häußler-Combe, U. und Pröchtel, P.: Ein dreiaxiales Stoffgesetz für Betone mit mittlerer und normaler Festigkeit. Beton- und Stahlbetonbau 100 (2005), S. 52-62.

[10] Harbord, R.: Finite Element Methode in der Baustatik und Baudynamik. Vorlesungsskript, Fachgebiet Statik der Baukonstruktionen, TU Berlin, 1997.

[11] Kaliszky, S.: Plastizitätslehre Theorie und technische Anwendungen. VDI-Verlag Düsseldorf, 1984.

[12] Kupfer, H.: Das Verhalten des Betons unter mehrachsiger Kurzzeitbelastung unter besonderer Berücksichtigung der zweiachsigen Beanspruchung. Deutscher Ausschuss für Stahlbeton, Heft 229.

[13] Kupfer, H., Hilsdorf, H. und Rüsch, H.: Behaviour of concrete under biaxial stresses. ACI-Journal 66 (1969), S. 656-666.

[14] Lemaitre, J.: A Course on Damage Mechanics. Springer-Verlag Berlin, Heidelberg, New York 1992.

[15] Lubarda, V., Krajcinovic, D., Mastilovic, S.: Damage model for brittle elastic solids with unequal tensile and compressive strength. Engng Fracture Mech., 49(5), S 681-697, 1994

[16] Meschke, G., Lackner, R., Mang, H. A.: An anisotropic elastoplastic-damage model for plain concrete. Int. J. Numer. Meth. Engng. 42, 703-727, 1998.

[17] Meyer, R.: Mehraxiales Werkstoffmodell für Beton mit einheitlichem Konzept im Vor- und Nachbruchbereich. Dissertation, TU Braunschweig, 1991.

[18] Perzyna, P.: Fundamental Problems in Visco-Plasticity. Advances in Applied Mechanics. 9, S. 243-377, 1966.

[19] Pieplow, K.: Untersuchungen zum Tragverhalten CFK-verstärkter Stahlbetonbauteile. Dissertation, TU Berlin, 2005.

[20] Pölling, R: Eine praxisnahe, schädigungsorientierte Materialbeschreibung von Stahlbeton für Strukturanalysen. Dissertation, Universität Bochum, Fakultät für Bauingenieurwesen, 2000

[21] Rasch, C.: Spannungs–Dehnungs–Linien des Betons und Spannungsverteilung in der Biegedruckzone bei konstanter Dehngeschwindigkeit. Berlin: Ernst & Sohn, 1962. (DAfStb Heft 154)

[22] Remmel, G.:(1994). Zum Zug- und Schubtragverhalten von Bauteilen aus hochfestem Beton. Heft 444, Deutscher Ausschuss für Stahlbeton.

[23] Reinhardt, H.W.: Fracture mechanics of an elastic softening material like concrete, Heron, 29(2), Delft, S. 1-42, 1984.

[24] Reyher, B.: Zur Modellierung von Low Cycle Fatigue-Effekten bei zyklisch beanspruchten Stahlbauteilen. Dissertation, TU Berlin, 2005.

[25] Schickert G. und Winkler, H.: Versuchsergebnisse zur Festigkeit und Verformung von Beton bei mehraxialer Beanspruchung. Deutscher Ausschuss für Stahlbeton, Schriftenreihe Heft 227, Berlin: Ernst & Sohn, 1977.

[26] Steberl, R.: Berechnung stoßartig beanspruchter Stahlbetonbauteile mit endochronen Werkstoffgesetzen. Werner-Verlag GmbH; Düsseldorf.

[27] Sinha, B., Gerstle, K., Tulin, L.: Stress-strain relations for concrete under cyclic loading. ACI Journal, 61, S. 195-211, 1964

[28] Valente, I., Cruz, P. J. S.: Experimental analysis of perfobond shear connection between steel and lightweight concrete. Journal of Constuctional Steel Research 60 S. 465-479, 2004.

[29] van Mier, J.: Strain-Softening fo Concrete under Multiaxial Loading Conditions, Dissertation, TU Einhoven, Niederlande, 1984.